Chlorination of hydrogen-terminated silicon (111) surfaces

Sandrine Rivillon and Yves J. Chabal[a)]
Department of Chemistry and Chemical Biology, Rutgers University, Piscataway, New Jersey 08854

Lauren J. Webb, David J. Michalak, and Nathan S. Lewis
Division of Chemistry and Chemical Engineering, Noyes Laboratory, 127-72 California Institute of Technology, Pasadena, California 91125

Mathew D. Halls and Krishnan Raghavachari
Department of Chemistry, Indiana University, Bloomington, Indiana 47405

(Received 7 October 2004; accepted 20 December 2004; published 28 June 2005)

Infrared absorption spectroscopy was used to investigate the chlorination of hydrogen-terminated Si(111) surfaces by three different methods: (a) exposure to a saturated solution of phosphorus pentachloride (PCl_5) in chlorobenzene; (b) exposure to chlorine gas, $Cl_2(g)$, and (c) exposure to $Cl_2(g)$ under UV illumination. X-ray photoelectron spectroscopy and first principles model (clusters) calculations were used to explore the structure and dynamics of these surfaces. The infrared spectra exhibited sharp chlorine-related vibrations at 586 and 527 cm^{-1}. The narrow full width at half maximum of these vibrations for all three preparation methods indicated that all functionalization schemes produced a nearly complete monolayer of Cl with little surface roughening or introduction of step edges. The 527 cm^{-1} mode was at a much higher frequency than might be expected for the bending vibration of Si monochloride. Theoretical calculations show, however, that this vibration involves the displacement of the top Si atom parallel to the surface, subject to a relatively stiff potential, shifting its frequency to a value fairly close to that of the Si–Cl stretching mode on a Si(111) surface. © *2005 American Vacuum Society.*
[DOI: 10.1116/1.1861941]

I. INTRODUCTION

Halogenated silicon (Si) surfaces are potentially important for many electronic device applications because chlorine termination can provide a template for thin film growth on silicon. In particular, halogenated surfaces have been used to facilitate the growth of high-κ dielectrics, the attachment of self-assembled monolayers, or to produce simple organic layers for application in biotechnology.[1,2]

Chlorine (Cl) is the most studied halogen with regard to surface interactions. Chlorine has been introduced onto clean silicon surfaces using either vapor deposition under ultrahigh vacuum or by use of plasma etching methods.[3–9] X-ray photoelectron spectroscopy (XPS), Auger emission spectroscopy and low energy electron diffraction have indicated that such functionalization methods produce fully chlorinated silicon surfaces.[3,10] Chlorine absorbs with an initial sticking coefficient of ~0.1 on the thermodynamically stable clean Si(111)-7×7 surface, with the absorbed Cl existing in both weakly and strongly bound states. Mono-, di-, and trichloride species are produced at low temperatures (<400 °C), while the monochloride moiety is the only species that remains stable at higher temperatures.[3] The Cl atoms occupy sites on the Si(111)-7×7 surface with the Si–Cl bond oriented normal to the surface.[11] Such surfaces have also been studied extensively theoretically.[12–16]

Scanning tunneling microscopy (STM) has been particularly useful in the elucidation of the structural modifications induced by chlorine gas [$Cl_2(g)$] etching of Si(111)-7×7 at high temperatures.[7,8] Upon reaction with Si(111)-7×7, STM experiments have shown that reacted and unreacted sites can be differentiated at low chlorine coverage (well below a monolayer saturation). At higher Cl_2 exposure, chlorine penetrates the adatom structures and inserts itself between the adatom and the rest-atom layers. After saturation coverage and annealing (300 °C), the reconstructed 7×7 chlorinated surface remains, but increasing the temperature to 500 °C converts the surface to a 1×1 chlorinated surface. Etching of silicon surfaces using chlorine plasmas has also been explored.[7,17–19] The etching rate is greatly enhanced upon *simultaneous* impingement of reactive species (chlorine) and energetic ions (Ar^+), while the individual species do not etch the silicon substrate by themselves.

More recently, methods have been developed to chlorinate *hydrogen*-terminated silicon surfaces using ambient pressure processes which are much more amenable to industrial requirements.[20–25] These chlorination methods start from the wet-chemically prepared H-terminated silicon surface. Wet chemical silicon chlorination methods have been described in the liquid phase using phosphorus pentachloride (PCl_5) and a radical initiator as a Cl radical source.[21–26] Gas phase methods, either in the dark[27] or using UV light in a low pressure chamber,[24] have also been demonstrated. Relatively little structural characterization has been performed to date on such chlorinated Si surfaces. The goal of the work described herein was to use high-resolution XPS in combination with infrared absorbance spectroscopy (IRAS) to characterize the reaction of chlorine with hydrogen-terminated,

a)Author to whom correspondence should be addressed; electronic mail: yves@agere.rutgers.edu

atomically flat silicon (111) surfaces using these three different chlorination techniques (wet chemical and gas phase methods). The properties of the surfaces prepared by the various ambient pressure chlorination methods have been compared, and together with theoretical calculations provide evidence for the formation of a monochloride-terminated surface.

II. EXPERIMENT

A. Sample preparation

The silicon samples (3.8 cm × 1.5 cm × 0.05 cm) were cleaned according to standard cleaning procedures, consisting first of etching in a solution of de-ionized (DI) $H_2O:H_2O_2:NH_4OH$, (4:1:1 by volume) and then in a solution of DI $H_2O:H_2O_2:HCl$ (4:1:1 by volume). In both cases the solutions were heated for 10 min at 80 °C. The Si samples were thoroughly rinsed with DI H_2O after each step. This cleaning protocol removed organic and metallic contaminants and produced a clean, thin SiO_2 layer on the surface. Hydrogen termination was achieved by subsequent etching for 30 s in 50% HF(aq) followed by a 2 min etch in NH_4F(aq).[28] STM data have confirmed that etching Si(111) surfaces in this manner produces atomically flat terraces that are hundreds of angstroms in width, and that a majority of the step edges on such surfaces are one atomic layer in height.[29] The chlorination of these freshly prepared H-terminated Si surfaces was then performed using the three different methods described below.

1. Wet chemistry method

In a nitrogen, N_2(g),-purged glovebox, a few grains of benzoyl peroxide as a radical initiator were added to a saturated solution of PCl_5 in chlorobenzene. The H-terminated Si sample was then immersed for 45 min at (90±5) °C in this solution. The sample was rinsed with anhydrous tetrahydrofuran and anhydrous methanol, and was then removed from the glovebox for XPS and IRAS studies.

2. Gas phase method

The chlorination reaction was performed at atmospheric pressure in a clean stainless-steel reactor that was continuously purged with pure N_2(g) (O_2 impurity $<10^{-6}$ ppm). During the reaction, the chamber was maintained at (95±2) °C, and Cl_2(g) (Matheson, research purity, 99.999%) was introduced with purified N_2(g) as the carrier gas (Cl_2/N_2=0.3%, total flow rate=4.7 L min^{-1}). After the Cl_2(g) exposure, the reactor was once again purged for 30 min with N_2(g) before the sample was examined using IRAS.

3. UV/chlorine method

The photochlorination was performed at atmospheric pressure in the same reactor as described above. Ozone-free UV lamps (BHK Mercury analamps with a filter for the 185 nm radiation that would produce ozone) were placed inside the reaction chamber. The lamps were situated ~0.5 cm from either side of the silicon sample, and both sides of the silicon wafer were exposed to UV light of equal intensity. The UV lamps were operated for 1 h prior to the chlorination reaction, to allow any contaminants to outgas from the lamps. The lamps were shut off briefly during the addition of Cl_2(g) and N_2(g) to the experimental chamber (Cl_2/N_2=0.03%). The reaction was performed at room temperature by turning on the UV lamps for 1 min followed by a 30 min N_2(g) purge in the dark to remove any remaining Cl_2(g) before infrared experiments were performed.

B. Measurements

1. XPS measurements

XPS measurements on functionalized Si(111) surfaces were performed using an M-Probe XPS system that has been described previously.[22,23] Aluminum Kα x rays at 1486.6 eV illuminated the sample at an incident angle of 35° off the plane of the surface. Photoelectrons emitted along a trajectory 35° off the surface plane were collected by a hemispherical electron analyzer. The instrumental resolution was 0.7 eV. Samples were inserted via a quick-entry load lock from the N_2(g)-purged glovebox directly into the ultrahigh vacuum (UHV) system and were kept at a base pressure of $\leqslant 1\times10^{-9}$ Torr. All samples were sufficiently electrically conductive at room temperature that no compensation for charging effects was required. On each sample, a wide energy range "survey" scan of core photoelectrons from 1 to 1000 eV (binding energy) was collected to identify the chemical species present on the surface.

2. SXPS measurements

High-resolution soft XPS (SXPS) experiments were performed on beamline U4A at the National Synchrotron Light Source (NSLS) at Brookhaven National Laboratory.[30] The samples were introduced through a quick-entry load lock into a two-stage UHV system that was maintained at pressures $\leqslant 1\times10^{-9}$ Torr. The beamline had a spherical grating monochromator and an entrance slit width that selected photon energies between 10 and 200 eV with a resolution of 0.1 eV. The selected excitation energy was not calibrated independently because our work was principally concerned with shifts in the Si 2*p* binding energy of surface atoms relative to the bulk Si 2*p* peak, as opposed to the determination of absolute binding energies. Samples were illuminated at an incident energy of 140 eV, and the emitted photoelectrons were collected normal to the sample surface by a VSW 100 mm hemispherical analyzer that was fixed at 45° off the axis of the photon source. The beam intensity from the synchrotron ring was measured independently, and the data in each scan were normalized to account for changes in photon flux during the scan. No charging or beam-induced damage was observed on the samples during data collection. The limited range of excitation energies available at this beamline, although well-suited for high surface resolution Si 2*p* core level spectroscopy, precluded measurement of SXPS survey scans of the surface.

Determination of the monolayer coverage of Cl on the functionalized surface has been described in detail.[26] The electron mean free path, λ_{Si}, at this excitation photon energy (140 eV) was estimated to be 3.5 Å, consistent with earlier reported values of 3.2–3.6 Å under similar conditions.[31,32] The penetration depth of the measurement can be calculated from $l_{Si}=\lambda_{Si}\sin\theta$, where θ is the collection angle off the surface. Data presented here were collected at $\theta=90°$, so $l_{Si}=3.5$ Å. To identify features in the Si $2p$ region in addition to the Si $2p$ bulk peak, the background was determined using a Shirley fitting procedure[33–35] and was then subtracted from the original spectrum. The background-subtracted spectra were then processed to deconvolute, or "strip," the Si $2p_{1/2}$ peak from the spin-orbit doublet.[32,36] To perform this spin-orbit stripping procedure, the energy difference between the Si $2p_{3/2}$ and Si $2p_{1/2}$ peaks was fixed at 0.6 eV, and the Si $2p_{1/2}$ to Si $2p_{3/2}$ peak area ratio was fixed at 0.51.[22,32,36,37] The residual spectrum composed of Si $2p_{3/2}$ peaks was then fitted with a series of Voigt line shapes[38] that were 5% Lorentzian and 95% Gaussian functions.[23,37] Finally, a simple overlayer-substrate model was employed to calculate the monolayer surface coverage.[23,36,37]

3. Infrared absorption spectroscopy

Immediately after processing, the chlorine-terminated Si samples were placed into the $N_{2(g)}$-purged sample compartment of a Fourier transform infrared spectrometer (Nicolet Nexus 670). All spectra were recorded in transmission mode with an incident IR beam angle of 74° off normal (Brewster angle for silicon) between 450 and 4000 cm^{-1}, with a room temperature DTGS detector. To characterize the orientation of the Si–Cl vibration, the photon incidence angle of the IR beam was rotated from 74° off normal (Brewster angle maximizing the transmission of the component perpendicular to the surface) to 30° off normal (where the component parallel to the surface dominated the signal). This method minimizes the possible reflection interferences (which are more severe at normal incidence) and also optimizes the beam throughput, making possible the detection of small Si–Cl absorbance features. The H-terminated silicon surface was used as a reference to determine the absorbance of the chlorinated surfaces.

III. EXPERIMENTAL RESULTS

Survey-scan XPS data from a freshly etched H-terminated Si(111) surface [Fig. 1(a)] confirmed that the only observable peaks were the Si $2p$ signal at 99.9 binding eV and the Si $2s$ signal at 151.1 eV binding energy. The peaks observed at successive intervals of 17.5 eV on the higher binding energy side of the two principal peaks have been identified as plasmon loss features, characteristic of crystalline silicon samples.[39,40]

Figure 1(b) shows a similar survey scan for the Cl-terminated surface prepared by exposure of H-terminated Si(111) to a saturated solution of PCl_5. In addition to the expected bulk Si $2s$ and $2p$ peaks, Cl $2p$ and $2s$ peaks were observed at binding energies of 199.5 and 270.3 eV, respectively, and an O $1s$ peak was observed at a binding energy of 531.2 eV. The coverage of O was determined previously to be 1.4±0.6 ML on such samples.[26] No evidence (<0.02 ML detection limit of the instrument) for SiO_2 was observed by SXPS in the entire energy region examined [Fig. 2(a)].

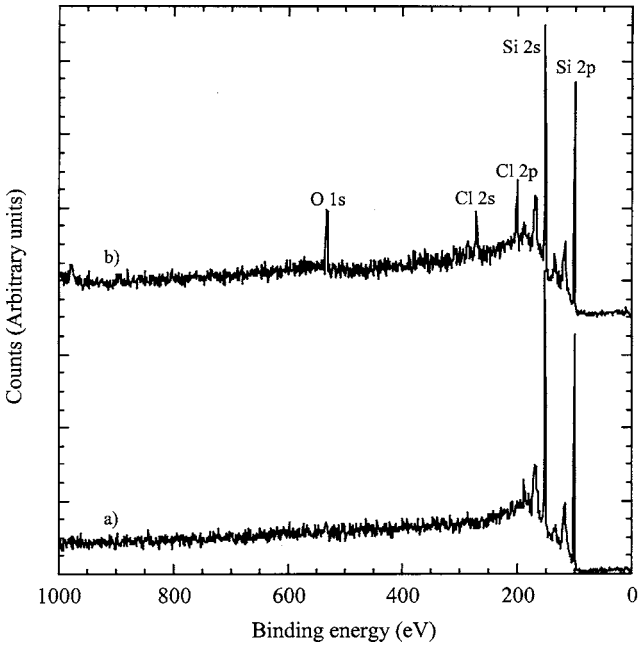

FIG. 1. Survey x-ray photoelectron spectra of functionalized Si(111) surfaces. (a) H–Si(111); (b) Cl–Si(111).

Figure 2 shows the SXPS peaks in the Si $2p$ region of the Cl–Si(111) surface. After the background had been removed, and the spectrum had been stripped of the Si $2p_{1/2}$ peak, a second Si $2p_{3/2}$ signal was observed at a binding energy +0.83 eV relative to the bulk Si $2p_{3/2}$ peak. This second peak was assigned to Si bound to one Cl atom. The magnitude and direction of this shift are consistent with expectations for a Si–Cl species because Cl (of electronegativity $\chi_p=3.16$)[41] is more electronegative than Si ($\chi_p=1.90$),[41] and electron density should thus be withdrawn from surface Si atoms to which Cl is bonded. Chlorine-terminated Si(111) surfaces prepared using UHV techniques have been reported previously to display Si $2p$ binding energy XPS peak shifts of 0.7–0.9 eV,[3,17,42–45] consistent with the observations described herein. The signal at +0.83 eV binding energy from the bulk Si $2p_{3/2}$ peak represented an equivalent coverage of 0.98 ML. A third peak, located at a binding energy +1.37 eV higher than the Si $2p_{3/2}$ peak, was much smaller in amplitude, and comprised 0.09 ML, or ~10% of the coverage observed for the monochlorinated Si feature. This binding energy shift is consistent with expectations for a Si atom bonded to two Cl atoms, which should exhibit a chemical shift approximately twice that of a Si monochloride species. The strength of the Si–Cl feature at +0.83 eV above the bulk Si $2p_{3/2}$ peak, as well as the presence of a small dichloride feature at +1.37 eV binding energy, may obscure the presence of a Si^+ suboxide, which would be found ~0.9 eV above the Si $2p_{3/2}$ bulk peak.

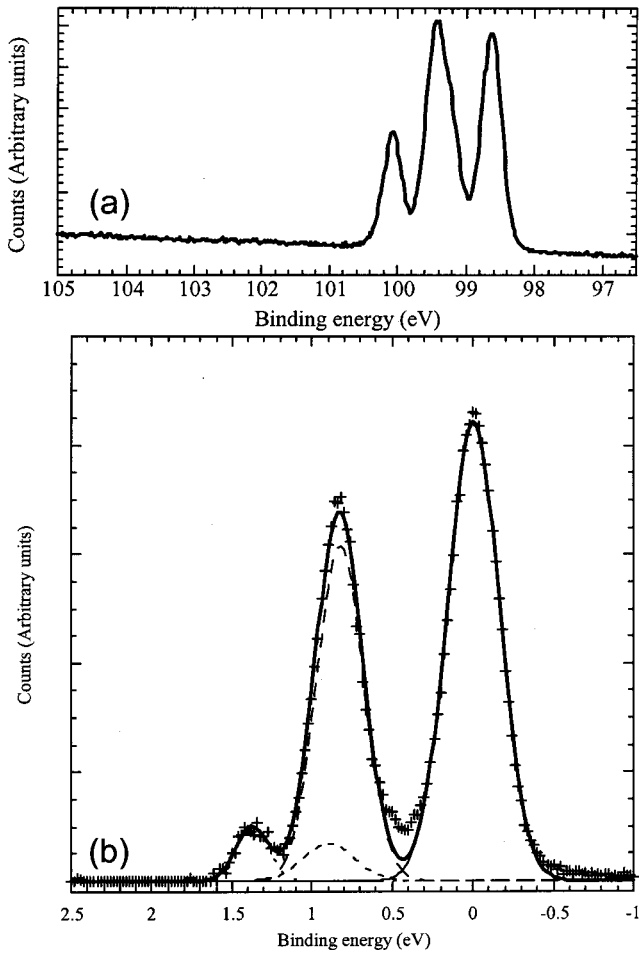

FIG. 2. SXPS spectra of the Si $2p$ region of a freshly prepared Cl–Si(111) surface and calculated background displayed relative to the binding energy of the bulk Si $2p_{3/2}$ signal. (a) The entire energy region that was examined, displayed as a function of the absolute binding energy measured before any data processing. (b) Background-subtracted Si $2p_{3/2}$ region curve fit. Crosses: raw data; thin solid line: center at 98.67 eV; long dashes: center at 99.49 eV; short dashes: center at 99.56 eV; dots; center at 100.03 eV; thick solid line: calculated curve fit.

Infrared absorption spectroscopy (IRAS) was used to provide direct information on the bonding and coverage of chlorine on such surfaces. Figure 3 shows the IR spectra of a silicon surface after chlorination using the same PCl_5 chlorination method. In this difference spectrum, using the H-terminated Si surface as background, absorbance features at 626 and 2084 cm^{-1}, corresponding respectively to the bending and stretching mode of H/Si(111),[28] appeared as negative features (loss of H). Sharp modes, at 586 and 527 cm^{-1}, were also observed and were located in a frequency range consistent with Si–Cl vibrations. The integrated area of the Si–H modes indicated that the loss of hydrogen was complete.[27] The assignment of the Si–Cl modes will be discussed below.

As shown in Fig. 4, all three chlorination methods clearly led to the same chlorinated surface under the optimum preparation conditions established for each surface. These results were strongly reproducible and for various samples studied with these three methods the same results were obtained. The

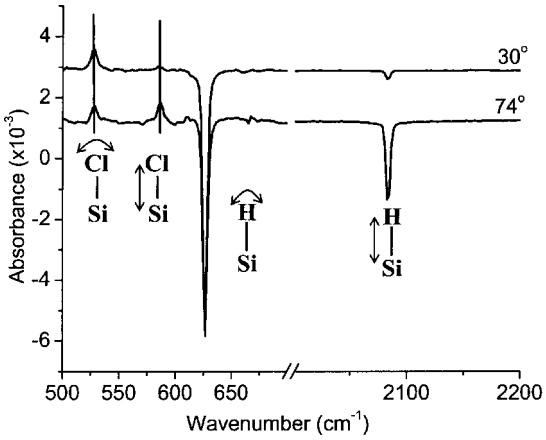

FIG. 3. Transmission infrared spectra (referenced to H-terminated Si) for two incidence angles (30° and 74°) of H/Si(111) after chlorination using the wet chemistry method.

gas phase and the wet chemistry chlorination methods produced surfaces having narrow IRAS features (full width at half maximum, FWHM, ~5 cm^{-1}) at 586 and 527 cm^{-1}, suggesting the formation of extended *homogeneous* domains of chlorine-terminated silicon (vide infra). In contrast, the photochlorinated surface exhibited a broader (FWHM ~10 cm^{-1}) mode that was also shifted slightly towards lower wave number (a ~6 cm^{-1} shift to 580 cm^{-1}). These two observations suggested that this surface was not fully covered with chlorine atoms. When comparing the Si–Cl features for the different processes, as well as the coverage experiments,[27] the peak position (frequency) of the mode is more revealing than the integrated area. As chlorine saturation was approached, the position of these two modes shifted. The overall behavior is typical of modes that are strongly affected by dipole-dipole interactions: the intensity of the mode parallel to the surface (527 cm^{-1}) is proportional

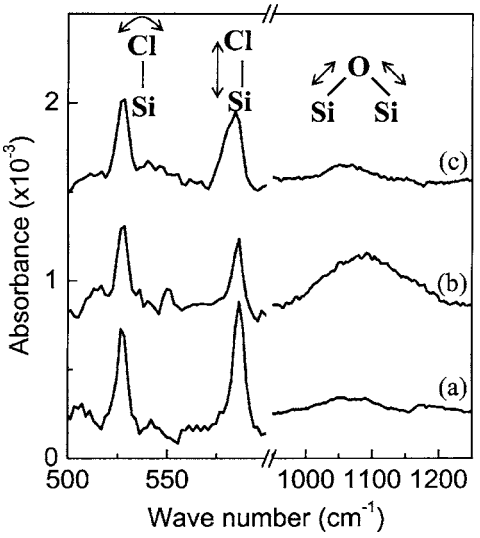

FIG. 4. Transmission infrared spectra (referenced to H-terminated Si) of Cl/Si(111) for different chlorination methods: (a) gas phase method, (b) wet chemistry, (c) UV light method.

to the coverage, while the mode perpendicular to the surface (586 cm^{-1}) is strongly blueshifted as the coverage increases, but its integrated intensity levels off (or even decreases slightly) due to electronic screening as the coverage approaches its saturation value.[27]

To determine whether oxygen had been incorporated into the surface structure, the region between 1000 and 1300 cm^{-1} was also examined using IRAS (Fig. 4). An absorbance feature at $\sim$1080 cm^{-1} indicated that some incorporation of oxygen into the silicon surface, in the form of Si–O–Si structures, had occurred. The integrated absorbance of this feature indicated that the amount of oxygen was $\sim$3% of a monolayer for the gas phase method and was $<\sim$15% of a monolayer for the wet chemical process. This relatively small level of contamination might have been produced during the wet chemical process of surface functionalization. In general, the gas phase method showed the least amount of oxygen contamination.

When the angle of the incident beam was moved from the Brewster angle towards the normal direction, to probe the orientation of the Si–Cl bond, the experiments (Fig. 3) clearly revealed that the intensities of the bands at 584 and 527 cm^{-1} varied in the same proportion as that of the Si–H stretching and Si–H bending modes. This behavior indicates that the dipole of the 584 cm^{-1} mode is oriented perpendicular to the surface but that the dipole of the 527 cm^{-1} band is oriented parallel to the surface.

IV. DISCUSSION

When a H-terminated Si(111) surface was exposed to a solution of PCl_5, the resulting Cl-terminated surface displayed a SXPS Si–Cl feature shifted 0.83 eV higher in binding energy than the bulk Si $2p_{3/2}$ peak, and represented an equivalent monolayer coverage of 0.98 ML. No evidence of contamination by silicon dioxide was observed, with no SiO_2 peaks at $\sim$+3.9 eV (for Si^{4+}) or at +2.5 eV (for Si^{3+}) relative to bulk Si.[32] The position of the surface Si–Cl feature made it difficult, however, to exclude the presence of a Si^+ peak, which would identify the presence of Si–O–Si features. To examine this possibility, the high-resolution SXPS spectrum of the Cl-terminated surface was also fitted with a fourth peak located +0.9 eV higher than the Si $2p_{3/2}$ bulk peak.[32] To avoid overfitting the data, this +0.9 eV peak was tightly constrained both in binding energy (+0.9 eV) and in overlayer coverage (<20%). The results, shown in Fig. 2, qualitatively demonstrate that the presence of Si–O–Si is not ruled out by the SXPS data. When a Si^+ peak was held at +0.9 eV above the Si $2p_{3/2}$ peak at 0.11 ML coverage, the location of the feature assigned to surface Si–Cl atoms did not change significantly (from +0.83 eV to +0.82 binding eV), but the calculated surface coverage fell from 0.98 to 0.92 ML. As expected, incorporation of this additional peak did not affect the remainder of the spectrum, with the location and equivalent surface coverage of the dichloride feature remaining at +1.37 eV and 0.09 ML, respectively.

Extended chains of Si–O–Si would result in Si^{2+} species on the surface. Experiments on the oxidation of the Cl-terminated surfaces exposed to air have shown that the Si^{2+} feature on such surfaces appears at 1.9–2.0 eV above the Si $2p_{3/2}$ bulk peak.[46] Examination of Fig. 2 clearly reveals that no signals were observed in this region, indicating that any Si–O Si moeities that developed during surface preparation existed in isolated structures and not in extended networks. The 1080 cm^{-1} feature observed by IRAS is consistent with the formation of isolated Si–O–Si in the subsurface. For H-terminated Si(100), the Si–O–Si asymmetric mode frequency increases from 990 to 1050 cm^{-1} with oxygen agglomeration (H–Si bound to 1, 2, or 3 oxygen atoms).[47] The situation should be significantly different if the silicon is terminated by a (much heavier) chlorine atom. In this case, the isolated oxygen atom located between two silicon atoms (e.g., Si–O–Si–Cl) will be characterized by an asymmetric stretch similar to that of isolated interstitial oxygen in bulk silicon (with an asymmetric stretch 1104 cm^{-1}). Therefore, the combination of SXPS data ruling out SiO_2 formation, and the presence of a broadband centered at 1080 cm^{-1} in the IRAS data, indicates that some oxygen had inserted between the top and second layer, remaining, however, isolated.

The infrared spectra also showed that the three chlorination methods (gas phase, wet chemistry and photochlorination) produced nominally identical Cl-terminated Si surfaces. The value of the FWHM (Fig. 4) indicated that the Si(111) surface was highly homogeneous, and the peak energy is consistent with the hypothesis that such surfaces are fully covered with chlorine atoms. Because the Cl-terminated surfaces were made from an atomically flat, H-terminated Si surface, the low FWHM and high homogeneity of the Si–Cl features indicates that the chlorination procedures did not lead to extensive roughening or pitting of the surface. The shifts observed for the chlorine modes as a function of $Cl_{2(g)}$ exposure reported previously,[27] in conjunction with the conclusion that the Si(111) surface remained atomically smooth, strongly suggests that the vibrations at 527 and 584 cm^{-1} are associated with a single chlorine species having two normal modes. Variation of the angle of incidence of the infrared beam relative to the surface plane showed that the 584 cm^{-1} mode was polarized perpendicular to the surface while the 527 cm^{-1} mode was polarized parallel to the surface. This set of observations cannot differentiate between monochloride or trichloride termination of the silicon. For the monochloride, the low frequency mode at 527 cm^{-1} would be associated with the Si–Cl bending vibration, while for the trichloride, this same feature would be associated with the asymmetric stretch of the $Si-Cl_3$ mode. Theoretical calculations were therefore used to distinguish between these two possible assignments.

A mixed approach was used in our theoretical investigations of the structures formed from the interaction of chlorine with the Si(111) surface. In previous work on H-terminated silicon, small cluster models that contained a single surface structural unit were found to be adequate to explain the adsorbate geometry as well as the associated IR spectra. However, two observations suggest that more complex structural models may be needed for Cl on Si(111). First, the coverage

dependence of the infrared spectra indicates that interactions between the adsorbate species are important. Second, the presence of a low frequency mode (527 cm^{-1}) suggests that coupling of the adsorbate vibrations to the substrate silicon motion may be important. An obvious strategy is to use techniques based on periodic boundary conditions, to properly represent the uniform coverage. However, techniques for the computation of force constants and vibrational frequencies are better developed in cluster models. Thus we have used a mixed approach in which the geometry of the surface was derived from a periodic unit cell calculation and the vibrational parameters were then calculated by using these geometrical parameters in a medium-sized cluster model. Previously, Ricca and Musgrave[48] have used a two-layer cluster model to investigate the bond energy for Cl desorption as well as the Si–Cl stretching frequency for the Cl-passivated Si(111) surface.

Two different structural models, a monochloride terminated surface and a trichloride terminated surface, were considered in the calculations. Qualitatively, the monochlorinated surface would have a higher stretching frequency and a lower bending frequency, while the trichlorinated surface would have symmetric and antisymmetric frequencies with the appropriate polarizations. Obvious strong steric interactions severely impact the trichlorinated surface model, and hence we first discuss the monochlorinated model.

The geometrical parameters were obtained from complete optimization using a periodic unit cell that contained four layers of silicon atoms. The surface silicons were terminated with the bound chlorine atoms while the bottom layer silicon atoms were terminated with hydrogen. A B-LYP gradient corrected density functional[49,50] with the polarized 6-31G* basis set[51] was used in these calculations. The optimized Si–Cl distance was found to be 2.11 Å, slightly shorter than the corresponding distance of 2.14 Å found for a hydrogen-terminated Si_{10} cluster [adamantane-cage model for Si(111)] containing a single surface chlorine. Note that the commonly used B3-LYP hybrid density functional is much more expensive for such periodic systems.

To analyze the vibrational modes of this system, the geometrical parameters obtained with the periodic unit cell were then used to generate truncated cluster models. To represent the local environment and interactions of surface chlorine atoms, a cluster model containing seven chlorine atoms was generated. The central surface chlorine was surrounded by six other chlorines in a lattice-like structure (Fig. 5). This cluster, $Si_{22}H_{21}Cl_7$, was the smallest cluster that produced a qualitatively correct description of the collective vibrations (*vide infra*) in the system. It contained seven first layer silicon atoms each attached to a chlorine, six second layer Si atoms, six third layer Si atoms, and three fourth layer Si atoms. All of the remaining broken Si–Si backbonds were terminated with hydrogen atoms to remove any artifacts that might arise from the presence of nonphysical unpaired spins. The overall point group symmetry of the cluster model was C_{3v}.

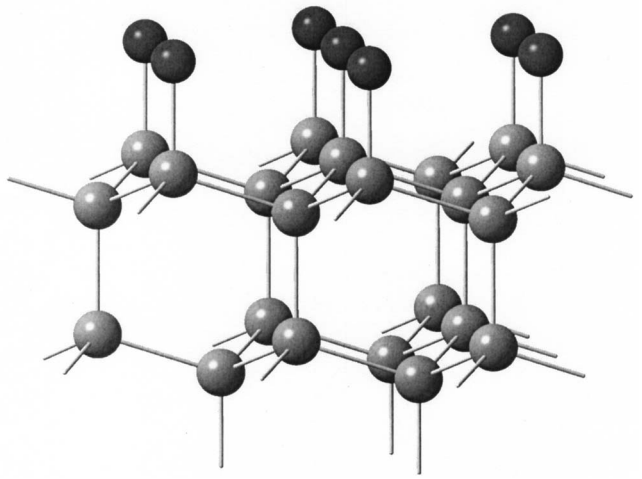

FIG. 5. Cluster model used at the B-LYP/6-31G* theoretical level.

The harmonic vibrational frequencies of the cluster model were calculated at the B-LYP/6-31G* theoretical level. The hydrogen atoms in the cluster were replaced with their isotopic analogs (D or T) in the vibrational analysis to prevent any nonphysical mixing of their vibrations with those of the Cl atoms. The lack of full periodicity in the cluster model, coupled with the presence of seven chlorine atoms, yielded many more vibrational modes than were seen experimentally. However, a careful investigation of the vibrational modes and their associated intensities indicated a clear emergence of collective vibrational modes even in such a small cluster model. For example, among the seven different Si–Cl stretching vibrations in our cluster model, a collective vibration, polarized perpendicular to the surface, occurred at 552 cm^{-1}. This vibration occurred at the highest frequency and had an intensity more than twice that of all the other six modes combined, clearly indicating that this vibration was emerging as the allowed surface stretching mode. In a similar manner, a parallel mode was calculated at 494 cm^{-1} (belonging to the degenerate "*e*" representation of the C_{3v} point group), and this mode emerged as a bending vibration with a strong intensity. However, this mode was dominated by the motion of the surface silicon atoms parallel to the surface and had only a small component associated with the surface-bound chlorine atoms. The calculations suggest that this behavior can be ascribed to the lighter mass of silicon as compared to chlorine. Thus, though this is a "bending" mode, the parallel motion of surface silicon atoms in their relatively stiff potential shifts the frequency to a value fairly close to that of the stretching mode. Though this bending mode is submerged in the lattice phonons, it has a strong intensity and is clearly associated with the surface. A low-intensity bending mode associated mostly with chlorine atom motion was also evident. This mode was calculated to occur at a much lower frequency ($\sim$100 cm^{-1}), which was beyond the range for which experimental data could be collected.

The emergence of two strong surface modes, a perpendicular mode at 552 cm^{-1} and a parallel mode at 494 cm^{-1}, is in excellent agreement with the experimental observations.

Hence we assign the mode at 586 cm^{-1} to a Si–Cl stretching motion and the mode at 527 cm^{-1} to a bending motion. Our calculated value of 552 cm^{-1} for the Si–Cl stretching mode is in good agreement with that obtained by Ricca and Musgrave[48] (538 cm^{-1}) at the B3-LYP/6-31G* level using a two-layer cluster model. The slightly low values of our computed frequencies relative to the values observed experimentally may be due to the use of the B-LYP density functional or to the relatively small size of the clusters used to describe such collective vibrations. The convergence behavior of the collective surface vibrational modes is currently being investigated using larger cluster models.

Similar models were attempted in the periodic unit cell calculations for surface $SiCl_3$ groups. However, the trichlorinated surface configuration has very large steric repulsions. For example, the van der Waals radius[52] of chlorine is 1.8 Å, indicating that optimal distances between the chlorine atoms should be ~3.6 Å or larger. Since the Si–Si distance on the Si(111) surface is only 3.8 Å, even with best possible dihedral rotations, we could not generate reasonable configurations containing $SiCl_3$ groups on all surface silicon atoms. Alternatively, we started from cluster geometries similar to that shown in Fig. 5 and attached $SiCl_3$ groups to the seven surface silicon atoms. The resulting optimized structure (not shown) was highly distorted and was not a realistic surface configuration. A uniform trichlorinated Si(111) surface can therefore be ruled out based solely on steric considerations. Overall, in conjunction with the SXPS results, the data strongly suggest that the surface consists of monochloride species. The similar results obtained on Cl-terminated surfaces prepared through three different methods suggest that the same mechanism is potentially responsible for the functionalization of the H-terminated Si(111) surface in each case.

V. CONCLUSIONS

H-terminated silicon(111) surfaces can be fully chlorinated using various methods: gas phase, wet chemistry and UV chlorination. The infrared spectra showed that all three methods led to fully covered monochlorinated Si(111) surfaces. The vibrational modes on chlorinated surfaces observed at 586 and 527 cm^{-1} are assigned to the Si–Cl stretching vibration and to a high frequency Si vibration parallel to the surface related to Si–Cl bending, respectively. The trichloride termination of Si(111) surfaces is shown to be sterically prohibitive and no evidence for this surface species was observed in the infrared absorption and core level photoemission studies.

ACKNOWLEDGMENTS

This work was supported by the National Science Foundation (Grant Nos. CHE-0415652 and CHE-0213589, as well as providing a graduate research fellowship to L.J.W.) and by International Sematech (Contract No. #306106 with FEPS008). This research was carried out in part at the National Synchrotron Light Source, Brookhaven National Laboratory, which is supported by the U.S. Department of Energy, Division of Materials Sciences and Division of Chemical Sciences, under Contract No. DE-AC02-98CH10886. The authors thank Michael Sullivan for use of the $N_2(g)$-purged glovebox at the NSLS. The authors are grateful to Martin M. Frank, Fabrice Amy, Rhett T. Brewer and Eric Garfunkel for fruitful discussions.

[1] J. M. Buriak, Chem. Rev. (Washington, D.C.) **102**, 1271 (2002).
[2] G. D. Wilk, R. M. Wallace, and J. M. Anthony, J. Appl. Phys. **89**, 5243 (2001).
[3] R. D. Schnell *et al.*, Phys. Rev. B **32**, 8057 (1985).
[4] P. A. Coon *et al.*, J. Vac. Sci. Technol. A **10**, 324 (1992).
[5] J. E. Rowe, G. Margaritondo, and S. B. Christman, Phys. Rev. B **16**, 1581 (1977).
[6] J. A. Yarmoff *et al.*, J. Vac. Sci. Technol. A **10**, 2303 (1992).
[7] J. J. Boland and J. S. Villarrubia, Science **248**, 838 (1990).
[8] J. J. Boland and J. S. Villarrubia, Phys. Rev. B **41**, 9865 (1990).
[9] C. M. Aldao and J. H. Weaver, Prog. Surf. Sci. **68**, 189 (2001).
[10] J. V. Florio and W. D. Robertson, Surf. Sci. **18**, 398 (1969).
[11] P. H. Citrin and J. E. Rowe, Surf. Sci. **132**, 205 (1983).
[12] G. A. de Wijs, A. De Vita, and A. Selloni, Phys. Rev. Lett. **78**, 4877 (1997).
[13] S. Sakurai and T. Nakayama, Surf. Sci. **493**, 143 (2001).
[14] D. Humbird and D. B. Graves, Chem. Phys. Lett. **120**, 2405 (2004).
[15] S. M. Mohapatra *et al.*, Phys. Rev. B **38**, 12556 (1988).
[16] S. Sakurai and T. Nakayama, J. Cryst. Growth **237–239**, 212 (2002).
[17] K. H. A. Bogart and V. M. Donnelly, J. Appl. Phys. **86**, 1822 (1999).
[18] N. C. M. Fuller *et al.*, Appl. Phys. Lett. **82**, 4663 (2003).
[19] S. C. McNevin and G. E. Becker, J. Vac. Sci. Technol. B **3**, 485 (1985).
[20] A. Juang *et al.*, Langmuir **17**, 1321 (2001).
[21] A. Bansal and N. S. Lewis, J. Phys. Chem. B **102**, 4058 (1998).
[22] A. Bansal *et al.*, J. Phys. Chem. B **105**, 10266 (2001).
[23] L. J. Webb and N. S. Lewis, J. Phys. Chem. B **107**, 5404 (2003).
[24] X.-Y. Zhu *et al.*, Langmuir **16**, 6766 (2000).
[25] J. Terry *et al.*, Nucl. Instrum. Methods Phys. Res. B **133**, 94 (1997).
[26] L. J. Webb *et al.*, J. Phys. Chem. B (in press).
[27] S. Rivillon *et al.*, Appl. Phys. Lett. **85**, 2583 (2004).
[28] G. S. Higashi *et al.*, Appl. Phys. Lett. **56**, 656 (1990).
[29] G. S. Higashi and Y. J. Chabal, *Silicon Surface Chemical Composition and Morphology* (Noyes, East Windsor, NJ, 1993).
[30] J. W. Keister *et al.*, J. Vac. Sci. Technol. A **17**, 1250 (1999).
[31] T. W. Pi *et al.*, J. Electron Spectrosc. Relat. Phenom. **107**, 163 (2000).
[32] F. J. Himpsel *et al.*, *Core Level Spectroscopy at Silicon Surfaces and Interfaces* (Varenna: North-Holland, Amsterdam, 1988).
[33] A. Proctor and P. M. A. Sherwood, Anal. Chem. **54**, 13 (1982).
[34] D. A. Shirley, Phys. Rev. B **5**, 4709 (1972).
[35] G. Contini and S. Turchini, Comput. Phys. Commun. **94**, 49 (1996).
[36] F. J. Himpsel *et al.*, Phys. Rev. B **38**, 6084 (1988).
[37] J. A. Haber and N. S. Lewis, J. Phys. Chem. B **106**, 3639 (2002).
[38] P. M. A. Sherwood, edited by D. Briggs and M. P. Seah (Wiley, New York, 1990), Vol. 1, p. 555.
[39] K. L. Cheng *et al.*, Jpn. J. Appl. Phys., Part 1 **34**, 5527 (1995).
[40] C. D. Stinespring and J. C. Wormhoudt, J. Appl. Phys. **65**, 1733 (1989).
[41] L. C. Allen, J. Am. Chem. Soc. **111**, 9003 (1989).
[42] N. Layadi, V. M. Donnelly, and J. T. C. Lee, J. Appl. Phys. **81**, 6738 (1997).
[43] C. C. Cheng *et al.*, J. Vac. Sci. Technol. A **12**, 2630 (1994).
[44] T. D. Durbin *et al.*, Surf. Sci. **316**, 257 (1994).
[45] J. A. Yarmoff *et al.*, J. Vac. Sci. Technol. A **10**, 2303 (1992).
[46] L. J. Webb and N. S. Lewis (unpublished).
[47] K. T. Queeney *et al.*, J. Appl. Phys. **87**, 1322 (2000).
[48] A. Ricca and C. B. Musgrave, Surf. Sci. **430**, 116 (1999).
[49] A. D. Becke, Phys. Rev. A **38**, 3098 (1988).
[50] C. Lee, W. Yang, and R. G. Parr, Phys. Rev. B **37**, 785 (1988).
[51] W. J. Hehre *et al.*, *Ab Initio Molecular Orbital Theory* (Wiley, New York, 1987).
[52] L. Pauling, *The Nature of the Chemical Bond* (Cornell University Press, Ithaca, New York, 1960).